ELSEVIER

Journal of Organometallic Chemistry 513 (1996) 85–95

Journal of Organometallic Chemistry

High nuclearity ruthenium carbonyl cluster chemistry IV [1]. Reactivity of $[Ru_{10}(\mu\text{-H})(\mu_6\text{-C})(CO)_{24}]^-$ towards trimethylphosphite or bis(diphenylphosphino)acetylene; X-ray crystal structure of $[PPh_4][Ru_{10}(\mu\text{-H})(\mu_6\text{-C})(CO)_{22}\{P(OMe)_3\}_2]$

Marie P. Cifuentes [a], Mark G. Humphrey [b,*], Anthony C. Willis [c]

[a] *Department of Chemistry, University of New England, Armidale, NSW 2351, Australia*
[b] *Department of Chemistry, Australian National University, Canberra, ACT 0200, Australia*
[c] *Research School of Chemistry, Australian National University, Canberra, ACT 0200, Australia*

Received 17 July 1995

Abstract

Reaction of $[PPh_4][Ru_{10}(\mu\text{-H})(\mu_6\text{-C})(CO)_{24}]$ (**1a**) with two equivalents of trimethylphosphite at room temperature gives a mixture of the mono- (**2a**), bis- (**3a**), tris- (**4a**) and tetrakis- (**5a**) phosphite-substituted cluster anions $[Ru_{10}(\mu\text{-H})(\mu_6\text{-C})(CO)_{24-x}\{P(OMe)_3\}_x]^-$ ($x = 1$–4). Reaction of $[Ru_2(\mu\text{-H})(\mu\text{-NC}_5H_4)_2(CO)_4(NC_5H_5)_2][Ru_{10}(\mu\text{-H})(\mu_6\text{-C})(CO)_{24}]$ (**1b**) with ten equivalents of trimethylphosphite at room temperature gives the tetrakis-substituted anion $[Ru_{10}(\mu\text{-H})(\mu_6\text{-C})(CO)_{20}\{P(OMe)_3\}_4]^-$ as its $[Ru_2(\mu\text{-H})(\mu\text{-NC}_5H_4)_2(CO)_4\{P(OMe)_3\}_2]^+$ salt (**5c**). Cluster **3a** has been characterized by an X-ray structural study, which confirms that the phosphite ligands occupy apical sites in these clusters. Reaction of $[Ru_{10}(\mu\text{-H})(\mu_6\text{-C})(CO)_{24}]^-$ with 20 equivalents of trimethylphosphite in refluxing acetone leads to tetradecapping of the decaruthenium core and formation of $Ru_6(\mu_6\text{-C})(CO)_{13}\{P(OMe)_3\}_4$ (**6**). Reaction of **1b** with 0.5 equivalents of bis(diphenylphosphino)acetylene gives the linked icosaruthenium cluster dianion $[\{Ru_{10}(\mu\text{-H})(\mu_6\text{-C})(CO)_{23}\}_2(\mu\text{-Ph}_2PC{\equiv}CPPh_2)]^{2-}$ (**7b**); heating **7b** leads to loss of the phosphine rather than ligand-assisted condensation.

Keywords: Ruthenium; Carbonyl; Cluster; Crystal structure

1. Introduction

The chemistry of high nuclearity ruthenium clusters is not as well developed as that of the analogous osmium clusters; weaker metal–metal bonds in the former militate against the stability of such species [2], and few high yielding routes into the ruthenium system exist. We recently reported the synthesis of $[Ru_2(\mu\text{-H})(\mu\text{-NC}_5H_4)_2(CO)_4(NC_5H_5)_2][Ru_{10}(\mu\text{-H})(\mu_6\text{-C})(CO)_{24}]$ (**1b**) in excellent yield, together with its structural characterization [3], and have investigated its reactivity towards triphenylphosphine [4]. It is possible to synthesize the apically substituted derivatives $[Ru_2(\mu\text{-H})(\mu\text{-NC}_5H_4)_2(CO)_4(NC_5H_5)_2][Ru_{10}(\mu\text{-H})(\mu_6\text{-C})(CO)_{24-x}(PPh_3)_x]$ ($x = 1$–4) in a stepwise fashion; the identity of the monosubstituted cluster anion $[Ru_2(\mu\text{-H})(\mu\text{-NC}_5H_4)_2(CO)_4(NC_5H_5)_2][Ru_{10}(\mu\text{-H})(\mu_6\text{-C})(CO)_{23}(PPh_3)]$ has been crystallographically confirmed. More recently, we have examined ligand fluxionality on the parent cluster anion $[Ru_{10}(\mu\text{-H})(\mu_6\text{-C})(CO)_{24}]^-$ and the triphenylphosphine derivatives by ^{13}C EXSY experiments [1] and have delineated the hydride and carbonyl site exchange pathways in this system. We have now extended our studies of ligand exchange to the linear diphosphine $Ph_2PC{\equiv}CPPh_2$ [bis(diphenylphosphino)-acetylene, dppa] and trimethylphosphite; we report herein our results from this work, including the single-crystal X-ray diffraction study of $[PPh_4][Ru_{10}(\mu\text{-H})(\mu_6\text{-C})(CO)_{22}\{P(OMe)_3\}_2]$.

* Corresponding author.
[1] For Part III, see [1].

SSDI 0022-328X(95)05896-6

2. Results and discussion

2.1. Syntheses and characterization of $[PPh_4][Ru_{10}(\mu\text{-}H)(\mu_6\text{-}C)(CO)_{24-x}\{P(OMe)_3\}_x]$ ($x = 1$–4)

Addition of equimolar trimethylphosphite to a stirred solution of $[PPh_4][Ru_{10}(\mu\text{-}H)(\mu_6\text{-}C)(CO)_{24}]$ (**1a**) gave a mixture, including some unreacted starting material; addition of a further equivalent of the phosphite and work-up by thin layer chromatography gave four separable products, identified as the mono-substituted, bis-substituted, tris-substituted and tetrakis-substituted clusters $[PPh_4][Ru_{10}(\mu\text{-}H)(\mu_6\text{-}C)(CO)_{24-x}\{P(OMe)_3\}_x]$ [$x = 1$ (**2a**), 2 (**3a**), 3 (**4a**) or 4 (**5a**)] (Scheme 1) by a combination of IR, ^1H and ^{31}P NMR, fast atom bombardment (FAB) mass spectroscopy (MS) and satisfactory microanalyses. The IR spectra contain ν(CO) bands in the terminal carbonyl region only; no bridging carbonyls are evident. Clusters **2a**, **3a** and **4a** contain four or five IR-active bands in this region, but the higher symmetry derivative **5a** contains two bands only. The ^1H NMR spectra contain resonances in the appropriate ratios assignable to PPh_4 and $P(OMe)_3$ species, together with hydride resonances; the latter appear as doublets (J(HP) = 10 Hz) with coupling characteristic of *cis*-disposed phosphite, and a fairly constant 0.02 ppm upfield march on successive substitution. The ^{31}P NMR spectra contain resonances assignable to PPh_4 (24.9 ppm) together with resonances in the appropriate ratios for cluster-ligated phosphite; the resonances at low fields

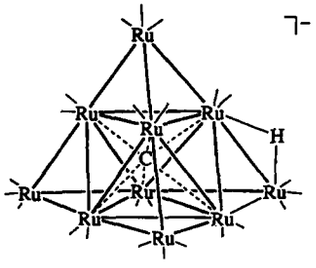

(1)

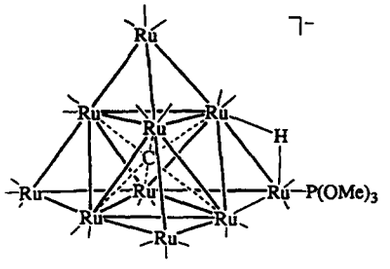

(2)

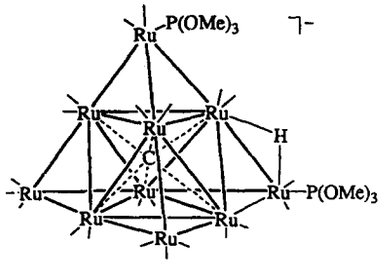

(3)

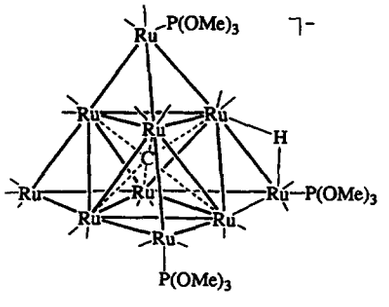

(4)

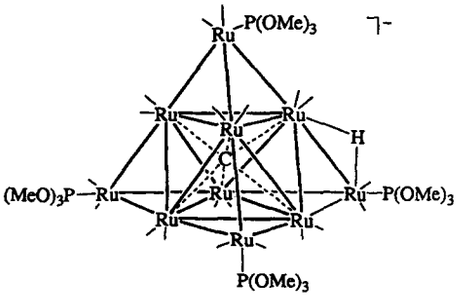

(5)

Scheme 1.

are assigned to the hydride-apex-containing phosphite. The identity of **3a** was confirmed by a structural study; it is the first crystallographically verified example of polysubstitution in the decaruthenium system.

2.2. X-ray structure of $[PPh_4][Ru_{10}(\mu\text{-}H)(\mu_6\text{-}C)(CO)_{22}\{P(OMe)_3\}_2]$ (3a)

An ORTEP plot of the major contributor (see below) to the anion is shown in Fig. 1, a summary of crystal and refinement data is found in Table 1, fractional coordinates are listed in Table 2, and selected bond lengths and angles are displayed in Table 3. The anion has the cluster core geometry of its precursor $[Ru_{10}(\mu\text{-}H)(\mu_6\text{-}C)(CO)_{24}]^-$ [3], and the mono(triphenylphosphine) derivative $[Ru_{10}(\mu\text{-}H)(\mu_6\text{-}C)(CO)_{23}(PPh_3)]^-$ [4], with the ten ruthenium atoms arranged as a tetracapped octahedron and a carbide ligand occupying the central cavity. The two phosphite ligands occupy apical coordination sites, with ten carbonyl ligands occupying the remaining apical coordination sites and 12 carbonyl ligands arranged two per edge ruthenium; Ru–CO and RuC–O distances are not unusual, and all Ru–C–O angles are approximately linear (168(3)–179(2)°) with no evidence of any semibridging interactions. No residues representing substantial hydride fractions were evident about the anion; in our two previously structurally characterized examples from this system, the hydride was not located crystallographically. Although one phosphite (that containing P(1)) is well behaved, the other is disordered and has been modelled over two sites (P(2), 75%; P(3), 25%): Refined distances and angles associated with phosphites containing P(2) and P(3) are relatively imprecise; deviations from idealized tetrahedral geometry about P(1) (Ru(9)–P(1)–O(23), 121.0(5)°; Ru(9)–P(1)–O(24), 119.6(5)°; Ru(9)–P(1)–O(25), 108.6(5)°) may result from repulsion owing to the hydride located on Ru(4)–Ru(9) and Ru(8)–Ru(9) (see below). The molecular geometry displayed in Fig. 1 is that of the major contributor.

Table 1
Crystallographic data for $[PPh_4][Ru_{10}(\mu\text{-}H)(\mu_6\text{-}C)(CO)_{22}\{P(OMe)_3\}_2]$ (3a)

Chemical formula	$C_{53}H_{39}O_{28}P_3Ru_{10}$
Formula weight	2227.5
Crystal system	Triclinic
Space group	$P\bar{1}$
a (Å)	14.187(2)
b (Å)	15.795(2)
c (Å)	16.937(2)
α (°)	95.44(1)
β (°)	106.91(1)
γ (°)	105.35(1)
V (Å^3)	3440.4(9)
Z	2
d_{calcd} (g cm^{-3})	2.150
μ (Cu Kα) (cm^{-1})	186.0
T (°C)	20(1)
Crystal dimensions (mm)	0.03×0.17×0.30
X-radiation	Cu Kα
λ (Å)	1.5418
Data range 2θ (°)	4–120
Number of unique data	10206
Number of data refined	6929 ($I > 3\sigma(I)$)
Number of variables	455
Number of restraints	22
R [a]	0.059
R_w [b]	0.057
Goodness of fit [c]	4.13
$F(000)$	2132

[a] $R = \Sigma \| F_o \| - \| F_c \| / \Sigma | F_o |$.
[b] $R_w = [\Sigma w(| F_o | - | F_c |)^2 / \Sigma (wF_o^2)]^{1/2}$.
[c] Goodness of fit $= [\Sigma w(| F_o | - | F_c |)^2 /$(number of reflections − number of variables)$]^{1/2}$.

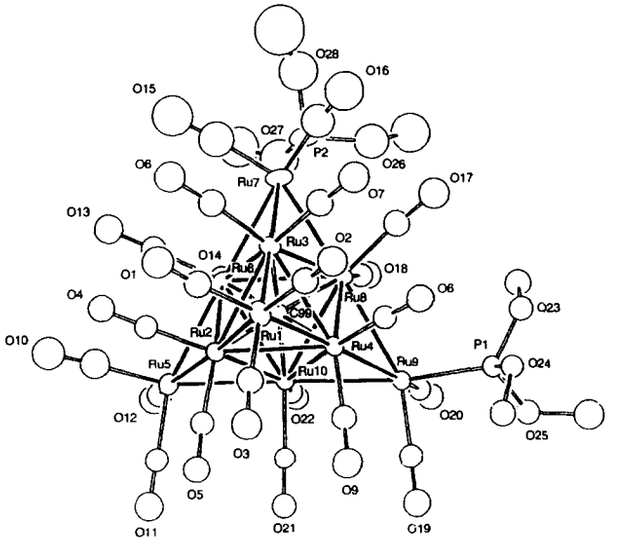

Fig. 1. Thermal ellipsoid diagram of the $[Ru_{10}(\mu\text{-}H)(\mu_6\text{-}C)(CO)_{22}[P(OMe)_3]_2]^-$ anion with labelling of selected atoms; carbon atoms have the same digit as the oxygen atoms to which they are bonded. Ellipsoids show 20% probability levels. The disordered atoms are shown only in their major orientation, and hydrogen atoms have been omitted.

As observed with other examples from the decaruthenium system, the Ru–Ru distances fall into two bands, with those for the central octahedral unit (2.823(2)–2.882(2) Å; average, 2.86 Å) being substantially longer than those to the apical ruthenium atoms (but excluding Ru(4)–Ru(9), 2.882(2) Å, and Ru(8)–Ru(9), 2.869(2) Å) which fall in the range 2.733(2)–2.821(2) Å (average, 2.78 Å). While the structure determination of $[Ru_2(\mu\text{-}H)(\mu\text{-}NC_5H_4)_2(CO)_4(NC_5H_5)_2][Ru_{10}(\mu\text{-}H)(\mu_6\text{-}C)(CO)_{23}(PPh_3)]$ [4] is inferior (in that it only establishes non-hydrogen atom disposition and connectivity), that of $[Ru_2(\mu\text{-}H)(\mu\text{-}NC_5H_4)_2(CO)_4(NC_5H_5)_2][Ru_{10}(\mu\text{-}H)(\mu_6\text{-}C)(CO)_{24}]$ [3] permits assignment of the hydride ligand location by indirect means; the hydride induces substantial lengthening of the bond on which it

Table 2
Atomic coordinates and isotropic displacement parameters for the non-hydrogen atoms in $[PPh_4][Ru_{10}(\mu\text{-}H)(\mu_6\text{-}C)(CO)_{22}\{P(OMe)_3\}_2]$ (**3a**)

Atom	*x/a*	*y/b*	*z/c*	U/U_{eq}
Ru(1)	0.3191(1)	0.2627(1)	0.91520(8)	0.0704(6) [a]
Ru(2)	0.21857(8)	0.25381(7)	0.74697(7)	0.0517(5) [a]
Ru(3)	0.43827(9)	0.31981(8)	0.81807(8)	0.0629(5) [a]
Ru(4)	0.33497(9)	0.13389(8)	0.79648(7)	0.0524(5) [a]
Ru(5)	0.1258(1)	0.25289(8)	0.57871(8)	0.0629(5) [a]
Ru(6)	0.34061(9)	0.31732(8)	0.64380(8)	0.0587(5) [a]
Ru(7)	0.5568(1)	0.37805(9)	0.7157(1)	0.0913(7) [a]
Ru(8)	0.45675(8)	0.19515(7)	0.69206(7)	0.0546(5) [a]
Ru(9)	0.34129(8)	0.00965(7)	0.66344(7)	0.0515(5) [a]
Ru(10)	0.23513(8)	0.13273(7)	0.62172(7)	0.0471(4) [a]
C(1)	0.309(2)	0.368(1)	0.961(1)	0.102(6)
O(1)	0.308(1)	0.439(1)	0.989(1)	0.137(6)
C(2)	0.410(2)	0.259(1)	1.017(1)	0.098(6)
O(2)	0.467(1)	0.257(1)	1.084(1)	0.125(5)
C(3)	0.201(2)	0.199(1)	0.936(1)	0.099(6)
O(3)	0.127(1)	0.154(1)	0.943(1)	0.128(5)
C(4)	0.197(1)	0.360(1)	0.771(1)	0.074(5)
O(4)	0.185(1)	0.4307(9)	0.7860(8)	0.101(4)
C(5)	0.091(1)	0.187(1)	0.750(1)	0.076(5)
O(5)	0.012(1)	0.1409(9)	0.7522(8)	0.096(4)
C(6)	0.453(2)	0.436(1)	0.857(1)	0.102(6)
O(6)	0.457(1)	0.513(1)	0.877(1)	0.129(5)
C(7)	0.551(2)	0.321(1)	0.904(1)	0.100(6)
O(7)	0.622(1)	0.318(1)	0.961(1)	0.130(5)
C(8)	0.425(1)	0.119(1)	0.891(1)	0.076(5)
O(8)	0.488(1)	0.1073(9)	0.9519(9)	0.105(4)
C(9)	0.228(1)	0.042(1)	0.802(1)	0.085(5)
O(9)	0.158(1)	−0.012(1)	0.807(1)	0.123(5)
C(10) [b]	0.093(2)	0.3579(9)	0.584(2)	0.12(1)
O(10) [b]	0.068(2)	0.423(1)	0.586(2)	0.153(9)
C(11)	−0.006(1)	0.179(1)	0.563(1)	0.071(4)
O(11)	−0.087(1)	0.1343(9)	0.5541(9)	0.110(4)
C(12)	0.104(1)	0.241(1)	0.465(1)	0.087(5)
O(12)	0.092(1)	0.235(1)	0.394(1)	0.122(5)
C(13)	0.330(1)	0.429(1)	0.652(1)	0.087(5)
O(13)	0.321(1)	0.502(1)	0.6617(9)	0.116(5)
C(14)	0.345(1)	0.311(1)	0.536(1)	0.086(5)
O(14)	0.346(1)	0.305(1)	0.467(1)	0.118(5)
C(15)	0.562(3)	0.492(2)	0.723(2)	0.17(1)
O(15)	0.559(2)	0.566(2)	0.727(2)	0.22(1)
C(16)	0.682(2)	0.407(2)	0.796(2)	0.15(1)
O(16)	0.754(2)	0.418(2)	0.858(2)	0.21(1)
C(17)	0.589(2)	0.202(1)	0.755(1)	0.096(6)
O(17)	0.672(1)	0.198(1)	0.798(1)	0.132(5)
C(18)	0.476(1)	0.167(1)	0.592(1)	0.073(5)
O(18)	0.483(1)	0.1543(9)	0.5242(8)	0.100(4)
C(19)	0.228(1)	−0.087(1)	0.652(1)	0.075(5)
O(19)	0.159(1)	−0.1474(9)	0.6425(8)	0.104(4)
C(20)	0.345(1)	−0.030(1)	0.560(1)	0.064(4)
O(20)	0.3438(9)	−0.0559(8)	0.4925(8)	0.091(4)
C(21)	0.111(1)	0.045(1)	0.6070(9)	0.058(4)
O(21)	0.0349(9)	−0.0085(8)	0.6013(7)	0.081(3)
C(22)	0.225(1)	0.103(1)	0.511(1)	0.066(4)
O(22)	0.2219(9)	0.0859(8)	0.4405(7)	0.084(3)
C(99)	0.339(1)	0.2251(9)	0.7197(8)	0.047(3)
P(1)	0.4463(3)	−0.0697(3)	0.7197(3)	0.063(2) [a]
O(23)	0.5664(9)	−0.0349(7)	0.7345(7)	0.081(3)
C(23)	0.606(2)	−0.008(1)	0.668(1)	0.097(6)
O(24)	0.4630(8)	−0.0835(7)	0.8132(7)	0.072(3)
C(24)	0.378(2)	−0.124(1)	0.840(1)	0.093(6)
O(25)	0.4047(9)	−0.1659(7)	0.6642(7)	0.081(3)
C(25)	0.456(2)	−0.234(2)	0.684(1)	0.123(8)
P(2) [b]	0.6484(6)	0.3888(5)	0.6272(6)	0.117(5) [a]

resides, a "splaying back" of the adjacent carbonyls, and a concomitant "folding in" of the carbonyls on the adjacent Ru–Ru bond (which slightly lengthens this bond); the variation in carbonyl geometry is accessible by evaluating cisoid ligand angle sums (see below). Two Ru–Ru bonds are lengthened substantially in the structure of **3a**, it is possible that the hydride is situated on Ru(4)–Ru(9) for the major contributor (75%), and on Ru(8)–Ru(9) for the minor contributor (25%) (it is emphasized that this is a suggested interpretation of the structural data). The result then for the major contributor is a slight lengthening of the associated Ru(1)–Ru(4) bond (2.821(2) Å), a lengthening not seen for the minor contributor. Angle sums (L–Ru(a)–Ru(b) + Ru(a)–Ru(b)–L) for cisoid ligands lie in the range 185.9–199.6°, except for C(14)–Ru(6)–Ru(7) + Ru(6)–Ru(7)–P(2) (210.2°), C(17)–Ru(8)–Ru(9) + Ru(8)–Ru(9)–P(1) (214.9°) and C(8)–Ru(4)–Ru(9) + Ru(4)–Ru(9)–P(1) (213.5°); for cluster **3a** (not surprisingly), all large angle sums are associated with the phosphites, although P(2)–Ru(7)–Ru(8) + Ru(7)–Ru(8)–C(18) is anomalously low at 199.6°. Significantly, the larger angle sums are associated with the Ru(8)–Ru(9) and Ru(4)–Ru(9) linkages at which we believe the hydride is located. Overall, the result is not as clear cut as with $[Ru_2(\mu\text{-H})(\mu\text{-NC}_5H_4)_2(CO)_4(NC_5H_5)_2][Ru_{10}(\mu\text{-H})(\mu_6\text{-C})(CO)_{24}]$ (**1b**), but the spectroscopic (*cis*-ligated hydride and phosphite at apical ruthenium) and crystallographic (bond lengthening and splayed ligands, as observed in **1b**) data for **3a** permit the cautious suggestion that the hydride is possibly located on Ru(4)–Ru(9) (major contributor) and Ru(8)–Ru(9) (minor contributor).

Table 2 (continued)
Atomic coordinates and isotropic displacement parameters for the non-hydrogen atoms in $[PPh_4][Ru_{10}(\mu\text{-H})(\mu_6\text{-C})(CO)_{22}\{P(OMe)_3\}_2]$ (**3a**)

Atom	*x/a*	*y/b*	*z/c*	U/U_{eq}
O(26) [b]	0.700(2)	0.311(1)	0.622(1)	0.164(9)
C(26) [b]	0.751(4)	0.275(3)	0.584(3)	0.21(2)
O(27) [b]	0.590(2)	0.384(2)	0.532(1)	0.21(1)
C(27) [b]	0.572(4)	0.440(4)	0.507(3)	0.23(2)
O(28) [b]	0.746(2)	0.473(2)	0.651(2)	0.21(1)
C(28) [b]	0.795(7)	0.543(6)	0.687(5)	0.35(4)
P(3) [c]	0.037(2)	0.354(1)	0.571(1)	0.108(8)
O(29) [c]	−0.067(3)	0.328(3)	0.493(2)	0.1300 [d]
O(30) [c]	0.002(4)	0.377(3)	0.650(2)	0.1300 [d]
O(31) [c]	0.100(3)	0.448(2)	0.559(3)	0.1300 [d]
P(4)	0.9561(3)	0.2328(3)	0.0749(2)	0.056(2) [a]
C(29)	0.904(1)	0.2900(9)	0.1393(9)	0.055(4)
C(30)	0.929(1)	0.290(1)	0.225(1)	0.075(5)
C(31)	0.884(1)	0.332(1)	0.273(1)	0.091(6)
C(32)	0.813(1)	0.371(1)	0.232(1)	0.087(5)
C(33)	0.785(1)	0.372(1)	0.149(1)	0.079(5)
C(34)	0.830(1)	0.331(1)	0.101(1)	0.068(4)
C(35)	0.864(1)	0.1292(9)	0.0194(9)	0.055(4)
C(36)	0.759(1)	0.112(1)	0.006(1)	0.069(4)
C(37)	0.690(1)	0.030(1)	−0.043(1)	0.084(5)
C(38)	0.721(1)	−0.033(1)	−0.078(1)	0.083(5)
C(39)	0.825(2)	−0.016(1)	−0.064(1)	0.094(6)
C(40)	0.897(1)	0.064(1)	−0.015(1)	0.078(5)
C(41)	1.068(1)	0.211(1)	0.1412(9)	0.058(4)
C(42)	1.054(1)	0.146(1)	0.187(1)	0.082(5)
C(43)	1.138(2)	0.130(1)	0.246(1)	0.094(6)
C(44)	1.231(2)	0.180(1)	0.254(1)	0.104(6)
C(45)	1.253(2)	0.242(1)	0.207(1)	0.097(6)
C(46)	1.169(1)	0.261(1)	0.145(1)	0.083(5)
C(47)	0.984(1)	0.300(1)	0.000(1)	0.065(4)
C(48)	0.941(1)	0.267(1)	−0.085(1)	0.088(5)
C(49)	0.963(2)	0.324(2)	−0.140(2)	0.122(8)
C(50)	1.026(2)	0.407(2)	−0.109(1)	0.112(7)
C(51)	1.072(2)	0.441(1)	−0.028(1)	0.104(6)
C(52)	1.050(1)	0.387(1)	0.030(1)	0.088(5)

[a] Anisotropic displacement factor $U_{eq} = \frac{1}{3}\Sigma_i\Sigma_j U_{ij} a_i^* a_j^* \boldsymbol{a}_i \boldsymbol{a}_j$.
[b] Occupancy, 0.75.
[c] Occupancy, 0.25.
[d] Fixed isotropic displacement factor.

2.3. Reactivity of $[Ru_{10}(\mu\text{-}H)(\mu_6\text{-}C)(CO)_{24}]^-$ (1) towards excess phosphite

The decaruthenium hydrido anion **1** is available with an excellent yield as its $[Ru_2(\mu\text{-}H)(\mu\text{-}NC_5H_4)_2(CO)_4(NC_5H_5)_2]^+$ salt **1b**, although **1b** and phosphine-substituted derivatives seem somewhat less stable than the analogous $[PPh_4]^+$ cluster **1a** and its derivatives [1]. Reaction of **1b** with two equivalents of trimethylphosphite proceeded in an analogous fashion to **1a**, affording

Table 3
Selected bond lengths (Å) and angles (°) for $[PPh_4][Ru_{10}(\mu\text{-}H)(\mu_6\text{-}C)(CO)_{22}\{P(OMe)_3\}_2]$ (**3a**)

Anion bonds			
External Ru–Ru bonds			
Ru(1)–Ru(2)	2.762(2)	Ru(1)–Ru(3)	2.733(2)
Ru(1)–Ru(4)	2.821(2)	Ru(2)–Ru(5)	2.767(2)
Ru(3)–Ru(7)	2.804(2)	Ru(4)–Ru(9)	2.882(2)
Ru(5)–Ru(6)	2.781(2)	Ru(5)–Ru(10)	2.776(2)
Ru(6)–Ru(7)	2.804(2)	Ru(7)–Ru(8)	2.793(2)
Ru(8)–Ru(9)	2.869(2)	Ru(9)–Ru(10)	2.782(2)
Internal Ru–Ru bonds			
Ru(2)–Ru(3)	2.848(2)	Ru(2)–Ru(4)	2.858(2)
Ru(2)–Ru(6)	2.869(2)	Ru(2)–Ru(10)	2.823(2)
Ru(3)–Ru(4)	2.848(2)	Ru(3)–Ru(6)	2.864(2)
Ru(3)–Ru(8)	2.881(2)	Ru(4)–Ru(8)	2.875(2)
Ru(4)–Ru(10)	2.882(2)	Ru(6)–Ru(8)	2.882(2)
Ru(6)–Ru(10)	2.835(2)	Ru(8)–Ru(10)	2.869(2)
Ru–carbide bonds			
Ru(2)–C(99)	2.04(2)	Ru(3)–C(99)	2.01(1)
Ru(4)–C(99)	2.03(1)	Ru(6)–C(99)	2.03(1)
Ru(8)–C(99)	2.02(2)	Ru(10)–C(99)	2.01(1)
Ru–phosphite bonds			
Ru(5)–P(3)	2.28(2)	Ru(7)–P(2)	2.24(1)
Ru(9)–P(1)	2.257(5)		
Anion bond angles			
Ru(1)–Ru(2)–Ru(5)	177.03(6)	Ru(1)–Ru(3)–Ru(7)	178.83(7)
Ru(5)–Ru(6)–Ru(7)	177.32(8)	Ru(1)–Ru(4)–Ru(9)	174.77(6)
Ru(5)–Ru(10)–Ru(9)	178.92(6)	Ru(7)–Ru(8)–Ru(9)	176.24(6)
Ru(2)–Ru(1)–C(1)	100.8(7)	Ru(1)–Ru(2)–C(4)	90.5(5)
Ru(2)–Ru(5)–C(10)	102(1)	Ru(2)–Ru(5)–P(3)	107.4(6)
Ru(5)–Ru(2)–C(4)	88.2(5)	Ru(4)–Ru(1)–C(2)	105.4(8)
Ru(1)–Ru(4)–C(8)	80.5(6)	Ru(9)–Ru(4)–C(8)	104.6(6)
Ru(4)–Ru(9)–P(1)	108.9(1)	Ru(10)–Ru(9)–C(19)	97.7(6)
Ru(9)–Ru(10)–C(21)	89.4(5)	Ru(10)–Ru(5)–C(11)	98.8(6)
Ru(5)–Ru(10)–C(21)	89.5(5)	Ru(1)–Ru(4)–C(9)	95.8(7)
Ru(4)–Ru(1)–C(3)	101.3(7)	Ru(4)–Ru(9)–C(19)	102.0(6)
Ru(9)–Ru(4)–C(9)	85.2(7)	Ru(2)–Ru(1)–C(3)	94.9(6)
Ru(1)–Ru(2)–C(5)	94.1(5)	Ru(2)–Ru(5)–C(11)	99.9(5)
Ru(5)–Ru(2)–C(5)	88.6(5)	Ru(10)–Ru(5)–C(12)	101.3(7)
Ru(5)–Ru(10)–C(22)	90.1(6)	Ru(10)–Ru(9)–C(20)	99.3(6)
Ru(9)–Ru(10)–C(22)	89.6(6)	Ru(5)–Ru(6)–C(13)	88.1(6)
Ru(6)–Ru(5)–C(10)	100.8(6)	Ru(6)–Ru(5)–P(3)	117.7(4)
Ru(6)–Ru(5)–C(12)	101.5(6)	Ru(6)–Ru(7)–C(15)	93(1)
Ru(7)–Ru(6)–C(13)	93.2(6)	Ru(5)–Ru(6)–C(14)	89.0(6)
Ru(7)–Ru(6)–C(14)	93.2(6)	Ru(6)–Ru(7)–P(2)	117.0(2)
Ru(3)–Ru(7)–C(15)	102(1)	Ru(7)–Ru(3)–C(6)	89.2(8)
Ru(3)–Ru(1)–C(1)	101.2(8)	Ru(1)–Ru(3)–C(6)	90.9(8)
Ru(1)–Ru(3)–C(7)	88.4(8)	Ru(3)–Ru(1)–C(2)	105.8(8)
Ru(3)–Ru(7)–C(16)	97(1)	Ru(7)–Ru(3)–C(7)	92.7(8)
Ru(9)–Ru(8)–C(17)	104.5(6)	Ru(8)–Ru(9)–P(1)	110.4(1)
Ru(8)–Ru(7)–C(16)	110(1)	Ru(7)–Ru(8)–C(17)	79.2(6)
Ru(8)–Ru(7)–P(2)	104.3(2)	Ru(7)–Ru(8)–C(18)	95.3(5)
Ru(8)–Ru(9)–C(20)	101.5(5)	Ru(9)–Ru(8)–C(18)	85.2(5)

monosubstituted to tetrakis-substituted clusters, with the last mentioned in trace amounts. Stirring **1b** with ten equivalents of trimethylphosphite overnight gave good yields of the tetrakis-substituted anion $[Ru_{10}(\mu\text{-}H)(\mu_6\text{-}C)(CO)_{20}\{P(OMe)_3\}_4]^-$ as its $[Ru_2(\mu\text{-}H)(\mu\text{-}NC_5H_4)_2(CO)_4\{P(OMe)_3\}_2]^+$ salt **5c**, identified by a combination of IR, ^1H and ^{31}P NMR and FAB MS. The ^1H NMR spectrum contains the characteristic doublet for the decaruthenium hydride with *cis*-ligated phosphite, together with a triplet at higher field (−13.85 ppm; $J(HP) = 12$ Hz) assigned to the hydride of the diruthenium cation. The ^{31}P NMR spectrum contains three resonances (ratio 1 : 3 : 2) assignable to the hydrido-apex phosphite, other phosphites of the decaruthenium anion, and phosphites of the diruthenium cation respectively.

The chemistry of the phosphite system is thus similar to that reported earlier for the triphenylphosphine system, but with enhanced reactivity. Whereas triphenylphosphine can be introduced in a stepwise manner at room temperature, trimethylphosphite affords mixtures of all four apically substituted derivatives on stirring at room temperature. Good yields of the tetrasubstituted derivative are attainable in both systems, concomitant with disubstitution of the diruthenium cation, but this reaction requires refluxing acetone in the triphenylphosphine system whereas it proceeds at room temperature with trimethylphosphite. Consideration of this enhanced reactivity led us to investigate reaction with phosphite under more forcing conditions. Reacting **1b** with 20 equivalents of trimethylphosphite in refluxing acetone gave a mixture of products from which the tetradecapped cluster $Ru_6(\mu_6\text{-}C)(CO)_{13}\{P(OMe)_3\}_4$ (**6**) was obtained (Scheme 2), characterized from its FAB MS and by comparison of its IR and ^1H NMR spectra with literature precedents [5]; disorder associated with phosphite ligands, coupled with a dearth of useful data consequent upon small specimen size, did not permit successful completion of an X-ray structural study [6].

The carbonylation of decaruthenium and decaosmium clusters has been reported. The cluster anion **1** (as the $[ppn]^+$ salt) is tetradecapped (1 atm CO; room temperature) to afford $[ppn][HRu_6(\mu_6\text{-}C)(CO)_{16}]$ and $Ru_3(CO)_{12}$ [7] and similar results were obtained with the dianion $[Ru_{10}(\mu_6\text{-}C)(CO)_{24}]^{2-}$, whereas the corresponding osmium dianion is resistant to CO at 1000–1500 atm and 200–250°C [8,9]. Complex **1** reacts with phosphite at room temperature, whereas the osmium dianion requires Os–Os cleavage by iodine to form

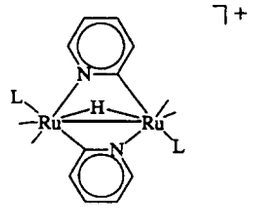

(b) L = NC_5H_5

(c) L = $P(OMe)_3$

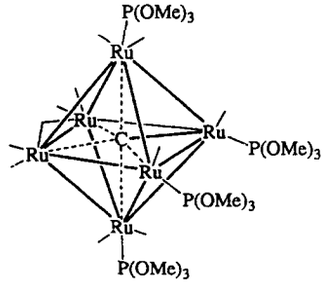

(6)

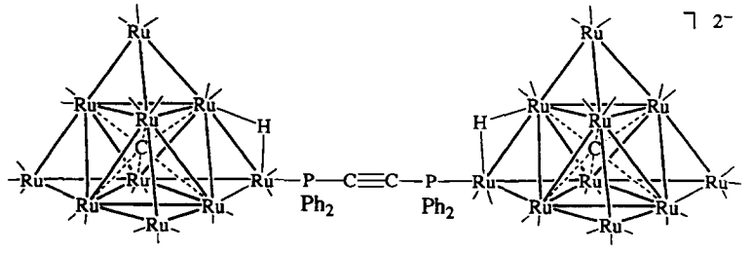

(7)

Scheme 2.

$Os_{10}(\mu_6\text{-C})(CO)_{22}(\mu\text{-I})_2$ before it will react with the phosphite in refluxing xylene, refluxing toluene proving insufficient [10].

2.4. Reactivity of 1 towards bis(diphenylphosphino)-acetylene

Bruce and coworkers have demonstrated that the cluster $[Ru_3(CO)_{11}]_2(\mu\text{-dppa})$ smoothly converts to $Ru_5(\mu_5\text{-}C_2PPh_2)(\mu\text{-}PPh_2)(CO)_{13}$ [11]. It was of interest to investigate whether or not this ligand-assisted cluster condensation methodology is applicable to the decaruthenium system. Reaction of **1b** with 0.5 equivalents of dppa gave a solution with the typical monosubstituted decaruthenium anion IR spectrum. The icosaruthenium cluster dianion $[\{Ru_{10}(\mu\text{-H})(\mu_6\text{-C})(CO)_{23}\}_2(\mu\text{-dppa})]^{2-}$ (**7b**) was obtained with a fair yield following chromatography and identified by a combination of IR, ^1H and ^{31}P NMR, FAB MS and satisfactory microanalyses. Significantly, the presence of a single decaruthenium hydride resonance (−11.90 ppm; $J(HP)$ = 9 Hz) and single dppa phosphorus resonance (18.1 ppm) are consistent with substitution occurring specifically at equivalent sites on the decaruthenium cores. The FAB MS has a band corresponding to $[M+H]^-$, together with bands assignable to $[HRu_{10}C(CO)_{23}(dppa)]^-$ (corresponding to loss of one decaruthenium core) and $[HRu_{10}C(CO)_{23}(Ph_2PC)]^-$ (corresponding to cleavage of the dppa ligand). Attempts were made to effect similar ligand-assisted cluster condensation to that achieved with $\{Ru_3(CO)_{11}\}_2(\mu\text{-dppa})$. Cluster **7b** is resistant to refluxing toluene (110°C), and reacted by loss of the dppa ligand in refluxing chlorobenzene (130°C) or *n*-butanol (116°C) to afford $[Ru_{10}(\mu\text{-H})(\mu_6\text{-C})(CO)_{24}]^-$; the reaction chemistry parallels results from the FAB MS (no condensation product, but rather expulsion of the decaruthenium cluster from the linked system), with the product isolated presumably resulting from scavenging of CO from another cluster.

3. Experimental details

The complexes $[PPh_4][Ru_{10}(\mu\text{-H})(\mu_6\text{-C})(CO)_{24}]$ [1], $[Ru_2(\mu\text{-H})(\mu\text{-}NC_5H_4)_2(CO)_4(NC_5H_5)_2][Ru_{10}(\mu\text{-H})(\mu_6\text{-C})(CO)_{24}]$ [3] and $Ru_3(\mu\text{-H})(\mu\text{-}NC_5H_4)(CO)_{10}$ [12] were synthesized according to the literature; the latter was purified by thin layer chromatography (TLC). Trimethylphosphite (Aldrich) and bis(diphenylphosphino)acetylene (Strem) were used as received. Petrol refers to the fraction with boiling point between 60–80°C. Reactions were carried out using Schlenk techniques [13] under an atmosphere of dry nitrogen; subsequent work-up was carried out without any precautions to exclude air.

The IR spectra were recorded using a Perkin–Elmer model 1600 Fourier transform spectrophotometer with CaF_2 optics. NMR spectra were recorded on a Varian Gemini 300 spectrometer (^1H spectra at 300 MHz and ^{31}P at 121 MHz) in acetone-d_6 unless otherwise stated. References for the ^1H NMR spectra were set to residual solvent peaks. The ^{31}P NMR spectra were recorded using a recycle delay of 40 s; they are reported relative to external 85% H_3PO_4 at 0.0 ppm and are proton decoupled. Mass spectra were recorded using a VG ZAB 2SEQ instrument (30 kV Cs^+ ions; current, 1 mA; accelerating potential, 8 kV; 3-nitrobenzyl alcohol matrix) at the Australian National University; peaks were recorded as m/z. TLC was on glass plates (20 × 20 cm) coated with Merck GF_{254} silica gel (0.5 mm) using 1 : 1 acetone : petrol as eluent.

3.1. Reaction of $[PPh_4][Ru_{10}(\mu\text{-H})(\mu_6\text{-C})(CO)_{24}]$ (1a) with $P(OMe)_3$

3.1.1. Two molar equivalents

Trimethylphosphite (350 μl of a 0.085 M solution in acetone, 0.030 mmol) was added to a stirred solution of **1a** (60 mg, 0.030 mmol) in acetone (10 ml). The presence of unreacted starting material was detected by a spot TLC; so a further portion of $P(OMe_3)$ was added (330 μl) and the mixture stirred for 1 h. Purification by TLC afforded four brown products identified as $[PPh_4][Ru_{10}(\mu\text{-H})(\mu_6\text{-C})(CO)_{23}\{P(OMe)_3\}]$ (**2a**) (R_f = 0.38; 5 mg, 0.024 mmol (8%)), $[PPh_4][Ru_{10}(\mu\text{-H})(\mu_6\text{-C})(CO)_{22}\{P(OMe)_3\}_2]$ (**3a**) (R_f = 0.33; 13 mg, 0.0060 mmol (20%)), $[PPh_4][Ru_{10}(\mu\text{-H})(\mu_6\text{-C})(CO)_{21}\{P(OMe)_3\}_3]$ (**4a**) (R_f = 0.25; 22 mg, 0.0095 mmol (32%)) and $[PPh_4][Ru_{10}(\mu\text{-H})(\mu_6\text{-C})(CO)_{20}\{P(OMe)_3\}_4]$ (**5a**) (R_f = 0.14; 10 mg, 0.0041 mmol (14%)).

3.1.2. Analytical data

2a: Anal. Found: C, 28.62; H, 1.39%; m/z M^- 1792. $C_{51}H_{30}O_{26}P_2Ru_{10}$ Calc.: C, 28.74; H, 1.42%; M^- 1792. IR (CH_2Cl_2): ν(CO) 2077w, 2045vs, 2019s, 2000s cm^{-1}. ^1H NMR: δ 8.03–7.97 (m, 4H, PPh_4), 7.89–7.85 (m, 16H, PPh_4), 3.89–3.82 (m, 9H, $P(OMe)_3$), −12.09 (d, $J(HP)$ = 10 Hz, 1H, $Ru_{10}H$) ppm. ^{31}P NMR: δ 130.5 (s, 1P, $Ru_{10}P$), 24.9 (s, 1P, PPh_4) ppm.

3a: Anal. Found: C, 28.53; H, 1.61%; m/z M^- 1888. $C_{53}H_{39}O_{28}P_3Ru_{10}$ Calc.: C, 28.58; H, 1.76%; M^- 1888. IR (CH_2Cl_2): ν(CO) 2066w, 2039vs, 2019s, 2011s, 1991m cm^{-1}. ^1H NMR: δ 8.03–7.99 (m, 4H, PPh_4), 7.89–7.85 (m, 16H, PPh_4), 3.85–3.78 (m, 18H, $P(OMe)_3$), −12.07 (d, $J(HP)$ = 10 Hz, 1H, $Ru_{10}H$) ppm. ^{31}P NMR: δ 133.4 (s, 1P, $Ru_{10}P$), 132.3 (s, 1P, $Ru_{10}P$), 24.9 (s, 1P, PPh_4) ppm.

4a: Anal. Found: C, 28.66; H, 2.08%; m/z M^- 1986. $C_{55}H_{48}O_{30}P_4Ru_{10}$ Calc.: C, 28.43; H, 2.08%; M^- 1986. IR (CH_2Cl_2): ν(CO) 2053w, 2019m, 2006s,

1983m cm^{-1}. ^1H NMR: δ 8.04–7.99 (m, 4H, PPh_4), 7.89–7.85 (m, 16H, PPh_4), 3.81–3.74 (m, 27H, $P(OMe)_3$), −12.05 (d, $J(HP) = 10$ Hz, 1H, $Ru_{10}H$) ppm. ^{31}P NMR: δ 135.9 (s, 1P, $Ru_{10}P$), 134.8 (s, 2P, $Ru_{10}P$), 24.9 (s, 1P, PPh_4) ppm.

5a: Anal. Found: C, 28.10; H, 2.28%; *m/z* M^- 2080. $C_{57}H_{57}O_{32}P_5Ru_{10}$ Calc.: C, 28.29; H, 2.37%; M^- 2080. IR (CH_2Cl_2): ν(CO) 2002vs, 1974m cm^{-1}. ^1H NMR: δ 8.05–7.97 (m, 4H, PPh_4), 7.89–7.85 (m, 16H, PPh_4), 3.77–3.69 (m, 36H, $P(OMe)_3$), −12.02 (d, $J(HP) = 10$ Hz, 1H, $Ru_{10}H$) ppm. ^{31}P NMR: δ 138.2 (s, 1P, $Ru_{10}P$), 137.0 (s, 3P, $Ru_{10}P$), 24.9 (s, 1P, PPh_4) ppm.

3.2. Reaction of $[Ru_2(\mu\text{-}H)(\mu\text{-}NC_5H_4)_2(CO)_4(NC_5H_5)_2][Ru_{10}(\mu\text{-}H)(\mu_6\text{-}C)(CO)_{24}]$ (1b) with $P(OMe)_3$

3.2.1. One equivalent

The reaction of **1b** with trimethylphosphite was carried out in the same manner as described for reaction of **1a** with the phosphite detailed above. A ^{31}P NMR spectrum of the reaction mixture indicated the presence of monophosphite- to tetrakisphosphite-substituted anions. Purification by TLC afforded the monophosphite- to trisphosphite-substituted anions in similar yields to those given in Section 4.1.1. For each product, the cation was identified as $[Ru_2(\mu\text{-}H)(\mu\text{-}NC_5H_4)_2(CO)_4(NC_5H_5)_2]^+$. The tetrakisphosphite-substituted anion was not isolated in sufficient amounts for characterization of the associated cation. The complexes were identified by comparison of the spectroscopic data with those of the $[PPh_4]^+$ analogues described above.

3.2.2. Ten molar equivalents

$Ru_3(\mu\text{-}H)(\mu\text{-}NC_5H_4)(CO)_{10}$ (120 mg, 0.18 mmol) in chlorobenzene (15 ml) was refluxed for 1 h. The mixture was cooled to room temperature and filtered, and the filtrate was reduced in volume to dryness. The residue **1b** was dissolved in acetone (20 ml). Trimethylphosphite (56 mg, 0.45 mmol) was added and the solution stirred at room temperature for 18 h. The solution was taken to dryness and subjected to TLC. The main green band was crystallized from acetone–*n*-butanol to afford a black microcrystalline solid identified as $[Ru_2(\mu\text{-}H)(\mu\text{-}NC_5H_4)_2(CO)_4\{P(OMe)_3\}_2][Ru_{10}(\mu\text{-}H)(\mu_6\text{-}C)(CO)_{20}\{P(OMe)_3\}_4]$ (**5c**) (59 mg, 0.021 mmol (47%)). Found: *m/z* M^- 2080; M^+ 720. $C_{66}H_{35}N_4O_{27}PRu_{12}$ calc.: M^- 2080; M^+ 720. IR (acetone): ν(CO) 2059w, 2032w, 2002vs, 1976m cm^{-1}. ^1H NMR ($CDCl_3$): δ 8.35 (m, 2H), 7.73 (m, 2H), 7.60–7.47 (m, 2H), 7.26–7.07 (m, 2H) (aryl H); 3.77–3.69 (m, 54H, $P(OMe)_3$), −12.01 (d, $J(HP) = 9$ Hz, 1H, $Ru_{10}H$), −13.85 (t, $J(HP) = 12$ Hz, 1H, Ru_2H) ppm. ^{31}P NMR: δ 138.2 (s, 1P, $Ru_{10}P$), 137.0 (s, 3P, $Ru_{10}P$), 134.4 (s, 2P, Ru_2P) ppm.

3.2.3. 20 molar equivalents

A mixture of **1b** (280 mg, 0.12 mmol) and trimethylphosphite (300 mg, 2.4 mmol) in acetone (15 ml) was heated at reflux for 20 min. Purification by TLC afforded a number of bands. The product of the second band was crystallized from CH_2Cl_2–hexane to afford red crystals identified as $Ru_6(\mu_6\text{-}C)(CO)_{13}\{P(OMe)_3\}_4$ (26 mg, 0.018 mmol (15%)). Found: *m/z* M^+ 1479. $C_{26}H_{36}O_{25}P_4Ru_6$ calc.: M^+ 1479. IR (CH_2Cl_2): ν(CO) 2033w, 1998vs, 1992vs, 1955(sh)m cm^{-1}. ^1H NMR: δ 3.79, 3.73 (2 × d, $J(HP) = 9$ Hz, 1 : 1, $P(OMe)_3$) ppm. ^{31}P NMR: δ 145.3, 138.7 (2 × t, $J(PP) = 7$ Hz, 1 : 1) ppm. (Literature [5] IR (cyclohexane); 2042w, 1999vs(br), 1965w, 1815vw cm^{-1}. ^1H NMR (solvent not stated): δ 3.75 (d), 3.69 (d) ppm.)

3.3. $[Ru_2(\mu\text{-}H)(\mu\text{-}NC_5H_4)_2(CO)_4(NC_5H_5)_2]_2[\{Ru_{10}(\mu\text{-}H)(\mu_6\text{-}C)(CO)_{23}\}_2(\mu\text{-}PPh_2C_2PPh_2)]$ (7b)

3.3.1. Synthesis

Dppa (15 mg, 0.037 mmol) was added to a solution of **1b** (170 mg, 0.073 mmol) in acetone (15 ml) and the mixture stirred for 5 min. An IR spectrum at this stage showed the typical monosubstitution pattern of the decaruthenium anion. Purification by TLC afforded one major dark band which was isolated and crystallized from CH_2Cl_2–hexane as a black microcrystalline solid (**7b**) (114 mg, 0.022 mmol (32%)).

3.3.2. Analytical data

Anal. Found: C, 29.68; H, 1.11, N, 1.94%; *m/z* $[M^{2-} + H]^-$ 3747. $C_{66}H_{35}N_4O_{27}PRu_{12}$ Calc.: C, 29.37; H, 1.21; N, 2.25%; M^{2-} 3746. IR (CH_2Cl_2): ν(CO) 2077 (w), 2047 (s), 2018 (m), 2002 (m) cm^{-1}. ^1H NMR: δ 8.61–8.53 (m, 12H), 8.04–7.47 (m, 40H), 7.08 (m, 4H) (aryl H); −11.90 (d, 2H, $J(HP) = 9$ Hz, $Ru_{10}H$), −10.74 (s, 2H, Ru_2H) ppm. ^{31}P NMR: δ 18.1 (s) ppm. Other negative-ion FAB MS signals: *m/z* $[\{HRu_{10}C(CO)_{23}\}(PPh_2C_2PPh_2)]^-$ 2064; $[(HRu_{10}C(CO)_{23})(PPh_2C)]^-$ 1866; $[HRu_{10}C(CO)_{21}]^-$ 1613.

3.3.3. Thermolyses of $[Ru_2(\mu\text{-}H)(\mu\text{-}NC_5H_4)_2(CO)_4(NC_5H_5)_2]_2[\{Ru_{10}(\mu\text{-}H)(\mu_6\text{-}C)(CO)_{23}\}_2(\mu\text{-}PPh_2C_2PPh_2)]$ (7b)

These are as follows.

(i) A solution of **7b** (17 mg, 0.0034 mmol) in chlorobenzene (10 ml) was heated at reflux for 40 min. An IR spectrum of the solution indicated the presence of $[Ru_{10}(\mu\text{-}H)(\mu_6\text{-}C)(CO)_{24}]^-$. The solution was taken to dryness and the product confirmed by ^1H NMR spectroscopy.

(ii) A similar reaction in *n*-butanol (10 ml) over 5 h also resulted in the formation of a mixture of $[Ru_{10}(\mu\text{-}H)(\mu_6\text{-}C)(CO)_{24}]^-$ with a small amount of $[Ru_{10}(\mu_6\text{-}C)(CO)_{24}]^{2-}$.

(iii) No reaction was observed when **7b** was heated in refluxing toluene over 1.5 h.

3.4. X-ray crystallography

A thin plate of $[PPh_4][Ru_{10}(\mu\text{-}H)(\mu_6\text{-}C)(CO)_{22}\{P(OMe)_3\}_2]$ (**3a**) was mounted on a Rigaku AFC6R diffractometer equipped with a graphite monochromator and attached to a Rigaku RU-200B rotating-anode X-ray generator with a copper target. 20 reflections were located and indexed on a primitive triclinic cell. Accurate lattice parameters were determined by least-squares analysis of the setting angles of 25 reflections $97° < 2\theta < 100°$ using $\lambda(\text{Cu K}\alpha_1) = 1.540\,60$ Å. Crystallographic data are given in Table 1. Intensity data were collected for reflections h, k, l with $2\theta \leqslant 120°$ (h, $0 \rightarrow 15$; k, $-17 \rightarrow 16$; l, $-18 \rightarrow 17$) using $\omega - 2\theta$ scans of width $(1.20 + 0.3 \tan \theta)°$ in ω at a rate of 16° min^{-1} in ω, weak reflections being rescanned up to three times more to ensure good counting statistics. Background counts were taken for one quarter of the scan time on each side of every scan. Three standards measured after every 150 reflections showed a 20% decrease in their intensities during data collection; data were corrected accordingly. Data were also corrected for absorption (transmission range, 0.081–0.582).

The structure was solved by direct methods [14] and difference Fourier techniques. A couple of unsatisfactory features were observed, however, for a simple ordered model. One was that, although the phosphite on Ru(9) was well behaved, the phosphite on Ru(7) gave atypically large displacement factors. It was also noted that carbonyl C(10) refined with a very small displacement factor and with a long Ru–C distance. It was therefore concluded that the second phosphite was disordered, residing on Ru(7) for approximately 75% of the time and on Ru(5) for 25%, with carbonyl groups alternating with them. Restraints [15,16] were placed on bond distances and angles within these groups as attempts were made to deconvolute the observed electron density; only the P and O atoms of the 25%-occupancy phosphite on Ru(5) were found, and the 25%-occupancy carbonyl on Ru(7) was not identified. Hydrogen atoms for the cation and the phosphite on Ru(9) were included in structure factor calculations at geometrically determined positions. Anisotropic displacement factors were used for Ru atoms and P atoms with occupancy greater than 0.7, while other atoms had isotropic displacement factors. Refinement was continued until all shift-to-error ratios were less than 0.05. Fig. 1 shows the second phosphite on its major site only and selected atom labelling.

Least-squares refinement was performed using full-matrix methods minimizing the function $\Sigma w(|F_o| - |F_c|)^2$ with $w = 1$ corresponding to unit weights. Maximum and minimum heights in a final difference map were 0.94(6) and −1.12(6) electrons Å^{-3} respectively with the major features lying close to Ru atoms or within the disordered phosphites. Data reduction and refinement computations were performed with XTAL3.2 [17]; atomic scattering factors for neutral atoms and real and imaginary dispersion terms were taken from *International Tables for X-ray Crystallography* [18]. Final parameters for the non-hydrogen atoms are given in Table 2 and selected interatomic distances and angles are given in Table 3. Tables of hydrogen atom coordinates and thermal parameters and a complete list of bond lengths and angles has been deposited with the Cambridge Crystallographic Data Centre.

Acknowledgements

We thank the Australian Research Council (ARC) for support of this work and Johnson–Matthey Technology Centre for the loan of ruthenium salts. MPC holds a UNE Postgraduate Research Scholarship. M.G.H. is an ARC Australian Research Fellow.

References

[1] M.P. Cifuentes, M.G. Humphrey, B.W. Skelton and A.H. White, *J. Organomet. Chem., 507* (1996) 163.
[2] M.P. Cifuentes and M.G. Humphrey, in E.W. Abel, F.G.A. Stone and G. Wilkinson (eds.), *Comprehensive Organometallic Chemistry II*, Vol. 7, Elsevier, Amsterdam, 1995, Chapter 16.
[3] M.P. Cifuentes, M.G. Humphrey, B.W. Skelton and A.H. White, *Organometallics, 12* (1993) 4272.
[4] M.P. Cifuentes, M.G. Humphrey, B.W. Skelton and A.H. White, *Organometallics, 14* (1995) 1536.
[5] S.C. Brown, J. Evans and M. Webster, *J. Chem. Soc., Dalton Trans.*, (1981) 2263.
[6] M.P. Cifuentes, M.G. Humphrey, B.W. Skelton and A.H. White, unpublished results.
[7] P.J. Bailey, G. Conole, B.F.G. Johnson, J. Lewis, M. McPartlin, A. Moule, H.R. Powell and D.A. Wilkinson, *J. Chem. Soc., Dalton Trans.*, (1995) 741.
[8] B.F.G. Johnson, J. Lewis, W.J.H. Nelson, M.D. Vargas, D. Braga, K. Henrick and M. McPartlin, *J. Chem. Soc. Dalton Trans.*, (1986) 975.
[9] T. Coston, J. Lewis, D. Wilkinson and B.F.G. Johnson, *J. Organomet. Chem., 407* (1991) C13.
[10] R.J. Goudsmit, P.F. Jackson, B.F.G. Johnson, J. Lewis, W.J.H. Nelson, J. Puga, M.D. Vargas, D. Braga, K. Henrick, M. McPartlin and A. Sironi, *J. Chem. Soc., Dalton Trans.*, (1985) 1795.
[11] M.I. Bruce, M.L. Williams, J.M. Patrick and A.H. White, *J. Chem. Soc., Dalton Trans.*, (1985) 1229.
[12] M.I. Bruce, M.G. Humphrey, M.R. Snow, E.R.T. Tiekink and R.C. Wallis, *J. Organomet. Chem., 314* (1986) 311.
[13] D.F. Shriver and M.A. Drezdzon, *The Manipulation of Air Sensitive Compounds*, Wiley, New York, 1986.
[14] G.M. Sheldrick, SHELXS-86, in G.M. Sheldrick, C. Krüger and R. Goddard (eds.), *Crystallographic Computing 3*, Oxford University Press, Oxford, 1985, p. 175.
[15] R. Olthof-Hazekamp, CRYLSQ, in S.R. Hall, H.D. Flack and J.M. Stewart (eds.), *The XTAL 3.2 Reference Manual*, University of

Western Australia, Nedlands, WA; University of Geneva, Geneva; University of Maryland, College Park, MD, 1992.
[16] J. Waser, *Acta Crystallogr., 16* (1963) 1091.
[17] S.R. Hall, H.D. Flack and J.M. Stewart (eds.), *The XTAL 3.2 Reference Manual*, University of Western Australia, Nedlands, WA; University of Geneva, Geneva; University of Maryland, College Park, MD, 1992.
[18] *International Tables for X-ray Crystallography*, Vol. IV, Kynoch, Birmingham, 1974, pp. 99–101, 149–150 (present distributor: Kluwer, Dordrecht, Netherlands).